JOURNAL OF GEOPHYSICAL RESEARCH, VOL. 87, NO. A12, PAGES 10,373–10,383, DECEMBER 1, 1982

Observations of Jupiter's Distant Magnetotail and Wake

W. S. KURTH[1], J. D. SULLIVAN[2], D. A. GURNETT[1], F. L. SCARF[3], H. S. BRIDGE[2], AND E. C. SITTLER, JR.[4]

In the period from mid-1980 to August 1981 the Voyager 2 plasma wave instrument occasionally detected clear signatures of Jovian nonthermal continuum radiation while the spacecraft was in the general downstream direction from Jupiter at distances of $5000 < R < 9000\ R_J$ (up to ~4.5 AU). The magnitude and duration of the events increased as Voyager 2 approached the nominal aberrated tail position in the spring of 1981 and also indicated a periodicity suggesting some solar wind control. Each event shows characteristics suggestive of electromagnetic radiation trapped within a low-density cavity. Supported with plasma observations, several of the events are characterized by a broad, moderately low density region surrounding a well-defined, very low density core. We conclude that this series of continuum radiation events is best interpreted as the passage of Voyager 2 through the extended magnetotail and wake of Jupiter. Although the analysis of the events does not lead to a unique and unambiguous understanding of the structure of the tail, we can speculate on the various allowed tail configurations consistent with the observations. There are many cases in which there is a significant difference in the estimated duration of a given event as defined by the plasma wave or plasma observations, which may be explained by dynamical processes in the tail such as a pinch-off or disconnection event similar to that observed in cometary plasma tails.

INTRODUCTION

The possibility of traversing Jupiter's distant magnetotail with Voyager 2 was first raised by *Scarf* [1979] and also by *Grzedzielski et al.* [1980]. Those predictions were confirmed by *Scarf et al.* [1981*b*] when a Jovian tail encounter at $R = 6200\ R_J$ was reported via measurements from the Voyager 2 plasma wave and plasma instruments. We now present the full set of observations of Jupiter's distant tail by the Voyager 2 plasma wave receiver and plasma science instrument as the spacecraft approached Saturn in late 1980 and early-to-mid 1981.

The primary signature of the distant Jovian magnetosphere or tail in the Voyager plasma wave data is nonthermal continuum radiation, which is generated within the Jovian magnetospheric cavity [*Scarf et al.*, 1979; *Gurnett et al.*, 1979; *Gurnett et al.*, 1980; *Scarf et al.*, 1981*a*, *b*]. The continuum radiation occurs over a broad spectral range, from a few hundred Hertz to several tens of kiloHertz; hence, a substantial portion of the spectrum lies below the nominal electron plasma frequency f_p^- in the solar wind at the heliocentric radial distance of Jupiter. Those waves with frequency less than the solar wind plasma frequency are trapped in the low-density regions of the magnetosphere and act as a pervasive tracer, enabling the Voyager plasma wave receiver to map the magnetosphere.

One of the more dramatic encounters with the Jovian tail in February 1981 has already been reported [*Scarf et al.*, 1981*b*]. Subsequent to the discovery of the February event we began a search of the plasma wave data for additional events, and this is a summary of the results of that search. In addition, we have made extensive use of plasma observations to supplement our understanding of the regions we have identified as the extended Jovian magnetotail and wake. For one event we compare, in detail, the continuum radiation observations, the plasma density profile, and the magnetic field data, and we uncover some striking differences, which may lead to evidence of dynamical processes occurring in the tail that have profound effects on the gross structure of the tail. Details of the plasma wave and plasma (PLS) instrumentation can be found in *Scarf and Gurnett* [1977] and *Bridge et al.* [1977], respectively. We have utilized analyses performed by the magnetometer team to increase our confidence in the identification of the continuum radiation events as tail signatures. Those magnetic field results are reported in *Lepping et al.* [1982].

OBSERVATIONS OF THE DISTANT JOVIAN MAGNETOTAIL

Figure 1 shows an example of the signature of a distant Jovian tail encounter as seen in the Voyager 2 plasma wave data. The amplitude of the electric field in each of six spectrum analyzer channels is plotted as a function of time. The height of the solid black area for each channel is proportional to the log of the 48-min average electric field strength, with the range between two channels representing about 100 db.

The event in Figure 1 is characterized by a gradual increase in amplitude of radiation at 1.78 kHz coupled with a broadening in spectral width to lower frequencies. During day 144 there is an abrupt intensification and drop in the low-frequency cutoff that lasts for about a day and forms the 'core' of the event. Over subsequent days the intensity decreases, and the lower-frequency cutoff of the continuum radiation returns to a few kiloHertz. Note that the abrupt, step-level changes, particularly in the 311-Hz channel, are operational mode-dependent changes in the noise environment of the spacecraft and are not natural signatures in the plasma wave environment.

We interpret the data in Figure 1 as continuum radiation trapped within a low-density region of the Jovian magneto-

[1] Department of Physics and Astronomy, The University of Iowa, Iowa City, Iowa 52242.
[2] Center for Space Research, Massachusetts Institute of Technology, Cambridge, Massachusetts 02139.
[3] TRW Defense and Space Systems Group, Redondo Beach, California 90278.
[4] Laboratory for Extraterrestrial Physics, Goddard Space Flight Center, Greenbelt, Maryland 20771.

Paper number 2A1387.
0148-0227/82/002A-1387$05.00

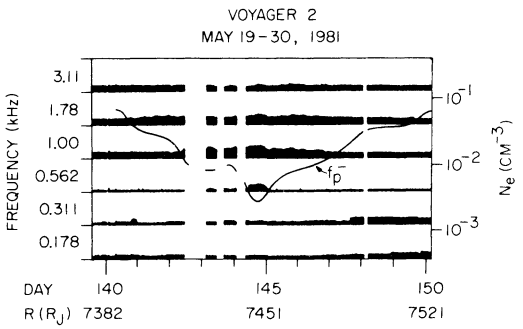

Fig. 1. Observations of nonthermal continuum radiation associated with Jupiter's magnetotail taken while Voyager 2 was ~7000 R_J downstream from Jupiter.

sheath and/or magnetotail. The radiation is very similar in amplitude and bandwidth to that shown in Figure 1 of *Kurth et al.* [1981] and also that studied by *Gurnett et al.* [1980] in the near-Jupiter tail lobes. The lower-frequency cutoff of the emission most likely indicates the local electron plasma frequency—the frequency at which electromagnetic radiation propagating in the ordinary mode cuts off. The density derived from this cutoff ($f_p^- = 8980\sqrt{n_e}$, where f_p^- is in Hertz and n_e is in electrons cm^{-3}) matches the density obtained from the plasma science instrument to within the accuracy of the measurements for most examples for which density comparisons have been made. Some potentially significant differences occur in the lowest-density regions, which will be discussed below.

A close examination of the 1.78- and 1.0-kHz channels in Figure 1 reveals some variations in intensity that one might believe to be periodic—the period being roughly 10 hours. On the basis of these data alone we could not defend the variations as being periodic, mainly because the variations do not continue for more than about three cycles. Examination of other events, however, does yield other examples of ~10-hour periodicities in the continuum radiation amplitude. A more striking case can be found in the 3.11-kHz channel of the event studied by *Scarf et al.* [1981*b*] (see Figure 1 of that paper). The 10-hour periodicity is extremely important in tying these remote observations to Jupiter since 10-hour variations are readily apparent in the continuum radiation amplitudes in the near-Jupiter magnetosphere. Plate 1 of *Scarf et al.* [1981*a*] shows the periodic variations near Jupiter very clearly. One might also expect to find similar periodicities in the plasma or energetic particle spectra during the tail encounters.

We have attempted to verify the connection of the ~10-hour periodicity in Figure 1, as well as that of Figure 1 of *Scarf et al.* [1981*b*], to Jupiter by comparing the System 3 central meridian longitude (CML) of the spacecraft at times when there are peaks in the radiation in both the distant and near-Jupiter observations. Analysis of the data in Plate 1 of *Scarf et al.* [1981*a*] shows the continuum radiation appearing to be modulated in time such that the peak intensity occurs not as a function of CML but at a time when the dipole field of Jupiter is at a particular orientation with respect to the sun. The analysis is further complicated by the appearance of two pulses during each 10-hour interval, seen most clearly during the Voyager 1 encounter. Preliminary analysis shows the main pulse occurs when the System 3 prime meridian is at a local time of ~18 hours (~90° past the noon meridian measured in the positive sense). The secondary peak occurs when the prime meridian is at a local time of ~9 hours.

The peaks in the 1.00- and 1.78-kHz channels in Figure 1 occur when the prime meridian is at a local time of ~8.5 hours (after correcting for the one-way light time from Jupiter). This corresponds very closely to the secondary peaks seen in Plate 1 of *Scarf et al.* [1981*a*], although it is not clear why only the secondary peaks are seen. The peaks observed by *Scarf et al.* [1981*b*] at 3.11 kHz occur when the prime meridian is near 21 hours local time. This is possibly related to the main pulse, but the agreement is not as good as in the previous case. We caution the reader that the foregoing analysis is only preliminary and that we do not understand the periodicities in the continuum radiation at this time. We merely wish to demonstrate the connection between the temporal variations of the distant continuum radiation events and those observed close to Jupiter. Further analysis of the temporal variations near Jupiter are the subject of another study.

Figure 2 shows data in a format similar to that in Figure 1, but for a longer interval. During the first part of April 1981, Voyager 2 was closest to the nominal aberrated tail position, and the data presented in Figure 2 indicate the spacecraft was detecting continuum radiation almost continuously during the period between days 92 and 109 of 1981. Several times during this interval the lower-frequency cutoff of the radiation extended to as low as 311 Hz, corresponding to an electron density of about 1.2×10^{-3} cm^{-3}. Each of these low-density regions is reminiscent of the core shown in Figure 1, but with durations ranging from a few hours up to a day.

The events shown in Figures 1 and 2 and also in Figure 1 of

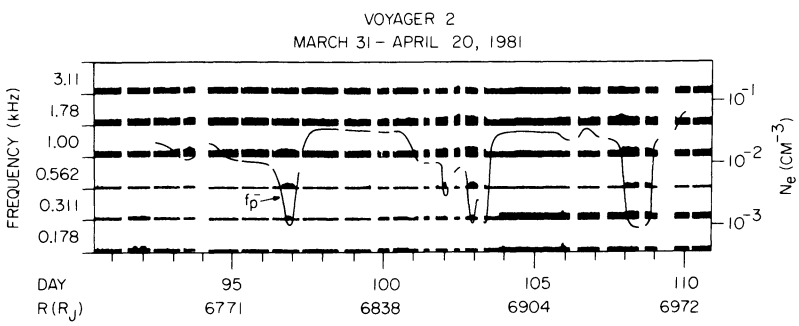

Fig. 2. Additional observations of continuum radiation gained while Voyager 2 was very close to the expected position of an extended Jovian magnetotail. The abrupt drops in the low-frequency cutoff of the radiation map extremely low density regions that probably represent actual encounters with the magnetotail.

TABLE 1. Voyager 2 Continuum Radiation Observations

Event	Year	Event Duration Start-Stop Day/SCET	Core Duration Start-Stop Day/SCET	Minimum f_p, kHz	Minimum n_e, cm^{-3}	R, R_J	ϕ^*, deg
1	1980	183/0130–188/0630	None	1.78	3.9×10^{-2}	3551	202.0
2	1980	209/2200–211/0830	None	3.11	1.2×10^{-1}	3802	199.9
3	1980	225/1330–225/1840	None	3.11	1.2×10^{-1}	3967	198.6
4	1980	303/0100–304/<1800	None	3.11	1.2×10^{-1}	4834	191.8
5	1980	324/0330–328/<1400	327/0130–328/0430	1.78	3.9×10^{-2}	5108	189.8
6	1980	347/>0700–350/1600	347/>1900–348/0330	1.00	1.2×10^{-2}	5349	188.0
			348/0900–348/<1500	1.00	1.2×10^{-2}	5355	188.0
9	1981	14/0800–15/1900	14/>1700–15/0145	1.00	1.2×10^{-2}	5735	185.3
			15/0320–15/0405	1.00	1.2×10^{-2}	5750	185.2
10	1981	16/1600–21/0600	20/1200–21/0600	1.78	3.9×10^{-2}	5821	184.7
12	1981	43/1500–53/1800	49/1700–51/<2030	0.562	3.9×10^{-3}	6194	182.2
			52/1800–53/0000	1.00	1.2×10^{-2}	6223	182.1
14	1981	66/0300–72/0430	68/1620–69/2130	1.00	1.2×10^{-2}	6432	180.7
			71/0130–72/0430	1.00	1.2×10^{-2}	6464	180.5
15	1981	92/>0400–94/<0440	None	1.00	1.2×10^{-2}	6746	178.7
16	1981	94/1500–98/0030	96/1400–97/0000	0.311	1.2×10^{-3}	6794	178.4
17	1981	100/0830–103/0830	101/2220–102/0030	0.562	3.9×10^{-3}	6864	178.0
			102/1740–103/0000	0.311	1.2×10^{-3}	6876	177.9
			103/0030–103/<0740	0.311	1.2×10^{-3}	6879	177.9
18	1981	106/1800–108/2030	107/2050–108/2030	0.311	1.2×10^{-3}	6950	177.5
19	1981	118/1430–119/0830	118/1900–119/0540	1.00	1.2×10^{-2}	7093	176.6
21	1981	140/0830–148/2000	144/0800–145/0000	0.562	3.9×10^{-3}	7446	174.6
22	1981	167/1630–170/0600	169/1500–170/0600	0.311	1.2×10^{-3}	7804	172.5
?24	1981	189/2200–190/1200	None	1.78	3.9×10^{-2}	8093	170.9
?25	1981	193/1700–201/0000	None	1.78	3.9×10^{-2}	8209	170.3
?26	1981	225/0630–230/1900	None	1.78	3.9×10^{-2}	8660	168.0

*Azimuthal angle in a Jupiter-centered system based on a plane parallel to the ecliptic measured in the right-hand sense from the solar direction.

Scarf et al. [1981*b*] are not the only detections of trapped continuum radiation at large distances from Jupiter. *Kurth et al.* [1981] studied observations of continuum radiation from Jupiter by both Voyager 1 and 2 as they left the Jovian system in the latter part of 1979 and early 1980. In that study, they interpreted some of the events as actual reentries into the Jovian magnetosphere and others as the detection of continuum radiation leaking out of the tail through low-density troughs in the solar wind that act as light pipes or wave guides. Table 1 is a list of all detections of continuum radiation by Voyager 2 since the interval studied by *Kurth et al.* [1981], that is, starting February 1, 1980. (For completeness we note here that one additional event was recorded by Voyager 1 that was not included in Table 1 of *Kurth et al.* [1981]. The new event occurred between ~1930 and ~2305 on day 157, 1980, when the spacecraft was at a distance of 6227 R_J and at an angle $\phi = 209.6°$, where ϕ is the azimuth angle in a right-handed Jupiter-centered system, with $\phi = 0$ oriented towards the sun.)

In addition to providing the overall duration of continuum radiation events, Table 1 also lists corelike structures, as described in the examples shown in Figures 1 and 2. A rather qualitative definition has been used in which well-defined extensions of the continuum spectrum to lower frequencies are considered to be cores. In general the cores have minimum densities at or below 1×10^{-2} cm^{-3}, although there are a few exceptions with somewhat greater minimum densities. The rather coarse frequency resolution available does not lend itself well to strict definition on the basis of minimum density alone. A more quantitative approach has been utilized in analyzing the plasma data, however, and that will be discussed below. For each event the minimum frequency at which the continuum radiation was detected and the corresponding electron density, assuming the cutoff occurs at the channel's center frequency, is listed. Also tabulated are the radial distance for each event (or core structure) and the azimuthal angle ϕ. We caution the reader that the last three entries in Table 1 are somewhat doubtful as far as their identification as continuum radiation is concerned. While the signature in the 1.78-kHz channel shows the usual slow variation in time of continuum radiation, wideband spectrograms taken during the last two intervals do not show the characteristic diffuse, broadband signatures of continuum radiation, but rather a sharp, narrow-band tone suggestive of spacecraft interference at about 1.75 kHz. Since the last three events are strictly confined to the 1.78-kHz channel, we suspect they may be spacecraft interference instead of continuum radiation. We note, however, that these events are accompanied by significant density dips and lobelike magnetic fields [*Lepping et al.*, 1982], and *Scarf et al.* [1982] have interpreted event 25 as a Jovian tail encounter on the basis of both plasma and plasma wave observations, hence, the disposition of these events is unclear. Notice in Table 1 that the events become more common, last longer, and extend to lower frequencies as the spacecraft passes through $\phi = 180°$.

Figure 3 is a plot of the position of Voyager 2 when it was detecting continuum radiation for the events starting with day 303, 1980, in Table 1. In the upper panel the trajectory is projected into the plane of Jupiter's orbit with the $-\hat{X}$ axis extending in the antisolar direction. A model of a possible Jovian magnetotail based on pre-Voyager considerations has been superimposed to put the observations into perspective. The shading represents a tail with a near-Jupiter diameter of

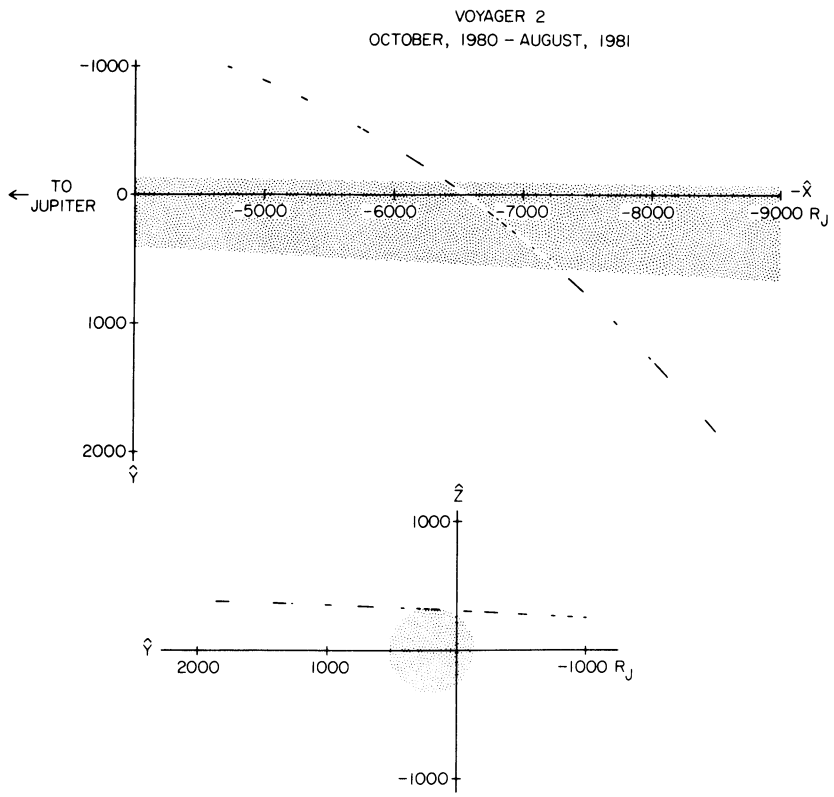

Fig. 3. A summary of the geometry for events listed in Table 1 that occurred when Voyager was very close to the antisolar direction. The shaded region represents a model tail that might have been proposed prior to the Voyager observations.

380 R_J, as suggested by *Kurth et al.* [1981], and with an aberration angle of about 1.8° (assuming a solar wind speed of 400 km/s). The model tail expands as the solar wind density decreases ($D \propto R$, where D is the diameter of the tail at a heliocentric radial distance R). The lower panel shows an orthogonal projection of the trajectory, this time as viewed from the antisolar direction.

Table 1 was constructed with plasma wave observations of continuum radiation only, since it has been assumed that the trapped radiation is a reliable signature of the tail. We supplement the continuum radiation table with a compilation of plasma observations of similar events or structures in Table 2 in order to begin to understand the plasma environment during the continuum radiation observations. Table 2 is constructed in a manner similar to Table 1 to facilitate cross comparison of the two data sets. In fact, the event designation numbers allow individual events identified by both the plasma wave and plasma science instruments to be compared directly, that is, event 5 in both tables is concerned with the same general time interval, and so on.

The PLS table was compiled from moment estimates of the ion density and speed. The densities and speeds are computed by integrating over the complete ion spectra

$$n_j = \sum_{i=1}^{16} \frac{I_{ij}}{eA_{\text{eff}}v_i} \qquad n = \frac{1}{3}\sum_{j=1}^{3} n_j$$

$$v_j = \frac{1}{eA_{\text{eff}}n_j}\sum_{i=1}^{16} I_{ij} \qquad v = \frac{1}{3}\sum_{j=1}^{3} v_j$$

where j is the index denoting sensors A, B, and C; I_{ij} is the current measured by sensor j at speed channel i; e is the unit of charge, and A_{eff} is the effective cross-sectional area of the main sensors. This method has the advantage of simplicity, and it reduces the time required to analyze such a large data set. It also discards no data (unless the quality is degraded by telemetry errors), even during extremely low density core regions. The errors introduced are relatively small; the error introduced by summing over alpha's is less than 20%, and background noise is ~0.005 cm^{-3} most of the time. Overall, the uncertainties are thought to be less than 50%.

Table 2 lists three sets of time periods. For an event to qualify as a 'tail' event, the density was required to be less than 0.03 cm^{-3} for a minimum of 6 hours. The overall event duration was then listed for the interval during which the density remained below 0.05 cm^{-3}. Core events were defined to be those time periods when the density fell below 0.01 cm^{-3}. The table also indicates the minimum density and whether or not the event was characterized by continuum radiation.

Where plasma is observable, the ion spectra are always solar windlike, consistent with a magnetosheath interpretation. In several core regions, however, the signal all but disappears in the PLS instrument, and these events correlate well with taillike field orientations (R. P. Lepping, private communication, 1982). These observations, then, are consistent with the picture obtained from the continuum radiation events that are characterized by deep core events (probable tail encounters) surrounded by moderately low density regions, herein referred to as wakes. Some of the events in Table 2 are highly structured, for example, events 15–17. These events show variability that is thought to be due to variations in either the solar wind ram pressure or solar wind directional changes or both.

TABLE 2. Voyager 2 PLS Low-Density Events

Event	Year	Event Duration Start-Stop Day/SCET	Continuum Radiation	$n_e < 3 \times 10^{-2}$ cm^{-3}	Core Duration, $n_e < 10^{-2}$ cm^{-3}	Minimum n_e, cm^{-3}	R, R_J	ϕ, deg
5	1980	323/2330–328/1615	Yes	326/2215–328/1415	None	2×10^{-2}	5094	189.9
6	1980	346/1145–355/1115	Yes	347/1900–350/1100 353/0015–354/0030 355/0030–355/0645	None	2×10^{-2}	5385	187.8
7	1980	363/0300–2/0100	No	364/0645–364/1415 365/1500–2/0000	None	5×10^{-3}	5561	186.5
8	1981	9/0445–11/0345	No	9/1000–9/1630 9/2015–10/1530	None	2×10^{-2}	5689	185.6
9–10	1981	12/1215–21/0830	Yes	14/0700–15/1815 17/0315–17/1400 20/1130–21/0730	None	1×10^{-2}	5772	185.1
11	1981	35/0130–38/1515	No	35/1430–36/0030 37/0130–38/1200	None	2×10^{-2}	6020	183.4
12	1981	43/2030–58/0015	Yes	48/0145–56/2100	51/0445–51/2045 52/1815–55/1845	1×10^{-3}	6197	182.2
13	1981	61/0745–62/0030	No	61/0745–62/0030	61/1000–62/0030	3×10^{-3}	6335	181.3
14	1981	66/0930–80/0615	Yes	66/1130–79/1500	67/0230–68/0430 68/1515–69/2145 71/0145–73/0115 73/1815–75/1330 76/1315–77/0900 77/1830–78/2045	2×10^{-3}	6486	180.4
15–17	1981	91/0000–103/0900	Yes	91/1515–103/0800	93/0215–97/0215 99/0045–99/1945 101/0145–102/0200 102/1715–103/0800	3×10^{-3}	6800	178.4
18	1981	104/1845–109/1630	Yes	107/0015–109/0500		1×10^{-2}	6935	177.6
19	1981	118/0945–120/0530	Yes	118/1500–119/0845	118/1815–119/0530	5×10^{-3}	7098	176.6
20	1981	121/2000–127/2230	No	124/0700–126/1045	124/0700–124/2315	3×10^{-3}	7174	176.1
21	1981	137/0415–151/0130	Yes	138/0045–139/0045 140/1930–151/0030	142/0615–147/2300	1×10^{-3}	7439	174.6
22	1981	161/0030–176/1800	Yes	162/0115–176/1045	164/1530–175/1615	1×10^{-3}	7788	172.6
23	1981	179/2345–186/1100	No	182/0845–183/1130 183/2200–185/1530	183/2300–185/1215	2×10^{-3}	7995	171.5
25	1981	195/1630–202/2100	Yes?	196/0545–196/1930 197/1100–197/1915 199/2030–202/1600	None	8×10^{-3}	8229	170.2
26	1981	222/0015–229/2000	Yes?	222/0430–223/1430 224/1010–226/0800 227/0145–228/0645	227/0600–228/0145	3×10^{-3}	8628	168.1

Comparison of Tables 1 and 2 leads to some interesting and significant conclusions. First, the PLS intervals tend to be broader than the continuum radiation events. In part, this may be due to low continuum radiation intensities near the beginning and end of the events or, perhaps, to a reduction in the solar wind density, which is a precursor for the appearance of an expanding tail. Another explanation for a disparity between the event durations in Tables 1 and 2 has rather interesting implications. Consider the event labeled 14 in both tables, which occurs when Voyager 2 was almost exactly in the antisolar direction from Jupiter. The overall duration of the continuum radiation event is much shorter (by several days) than the PLS event, which happens to be one of the longest events observed by PLS. The time of onset is very similar, but the continuum radiation disappears ~8 days before the density returns to a nominal value near 0.3 cm^{-3}.

The plasma wave observations, as well as plasma and magnetometer data for event 14, are shown in Figure 4. The continuum radiation, which is prominent in the upper panel near the beginning of the interval, is undetectable beyond day 72. The density profile shown in the next lower panel is derived from the PLS data and shows a broad low-density feature accentuated by more-or-less periodic rarefactions occurring every 2 days or so. The more prominent of these rarefactions are centered near days 67, 69, 71, 74, 76, and 78. In the third panel from the top, the magnetic field intensity is shown. For the entire low-density region the field is very weak, but is weakest in the lowest-density regions. The bottom panel shows the direction of the field. The angle β is 90° for a field aligned toward (or away) from Jupiter and is near 0° for the nominal interplanetary field direction. While the correlation is not exceptional, it is clear the nearly radial fields lie in the extremely low density regions. The field is in the usual interplanetary configuration ($\beta \approx 0°$) near the beginning and end of the event and during the higher-density intervals.

If one ignores the periodic rarefractions in the second panel of Figure 4, there is no apparent reason to expect the continuum radiation to disappear midway through the event. It is clear that lobelike magnetic fields accompany the low-density regions subsequent to day 72, and except for the lack of continuum radiation it is reasonable to call these regions taillike. We are compelled, however, to explain the abrupt disappearance of the continuum radiation, and, as we shall discuss in the next section, a simple way of 'turning off' the radiation is by inserting a high-density barrier between the spacecraft and the source of the radiation.

There are other examples of event 14 carried to an extreme. Several of the Table 2 events are apparently

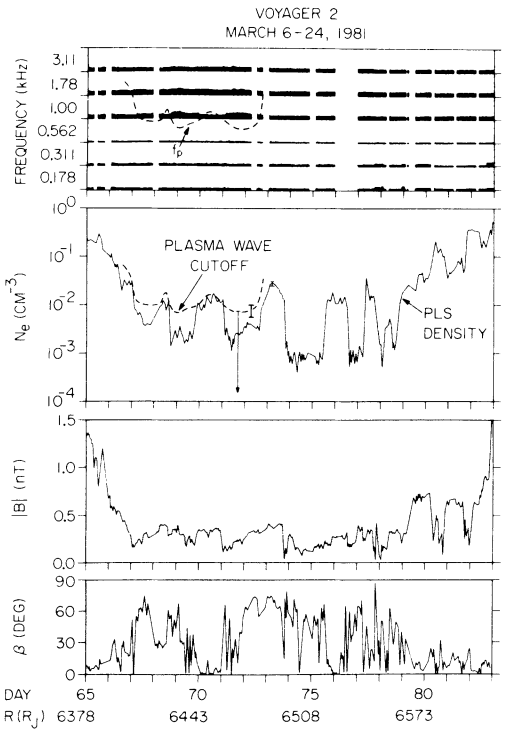

Fig. 4. A comparison of continuum radiation observations, plasma densities, and magnetic field intensities and directions for event 14 (see Tables 1 and 2). The plasma wave data in the upper panel show continuum radiation only to day 72, while the broad low-density feature, as seen in the PLS density profile, continues to day 82. The magnetometer data shows the deepest density depletions accompanied by very low magnetic field strengths and radially aligned (or anti-aligned) fields ($\beta \approx 90°$). The dashed line corresponds to a density profile that assumes that the low-frequency cutoff of the continuum radiation gives the local plasma frequency. The difference in the two density profiles within the lowest-density regions may be due to instrumental uncertainties (see error bars) or to a remote cutoff in the radio wave spectrum, in which case the local density could be much lower than implied by the dashed line. Note the quasi-periodic nature of the lowest-density intervals evident in both the plasma wave and PLS density profiles, which may be evidence of large-scale wave structure in the tail.

legitimate tail events as determined by the plasma observations and taillike field configurations (R. P. Lepping, private communication, 1982) but are not accompanied by continuum radiation at all. For these examples we must assume an explanation similar to that used for the event shown in Figure 4, but with the obstruction of the electromagnetic waveguide occurring prior to the spacecraft's entry into the tail region.

Returning our attention to the periodic variations apparent in Figure 4, we can make the following observation. The plasma wave receiver, the plasma instrument, and magnetometer all show evidence for temporal variations, although the effect is most dramatic in the PLS data. It is interesting to note that the density derived from the continuum radiation cutoff coincides with the density derived from the PLS instrument for the higher-density region, but in the density minima evident in both curves the densities obtained by PLS are significantly lower. Typical error bars are shown in Figure 4, which indicate the disparity in the minimum density measurements may be explained solely on the basis of measurement uncertainties. On the other hand, there is reason to believe the actual in situ densities as derived from the PLS observations are, indeed, lower than those implied by the continuum radiation cutoff. The obvious way to reconcile a real difference is to argue that the continuum radiation cutoff is imposed remotely by some intervening high-density region between the source and Voyager. The correlation of the low-density regions with low field intensities and nearly radially aligned fields requires consideration of entries into an actual taillike region and not simply a density variation in a sheathlike region. This, plus the periodic nature of the variation, suggests a wave possibly on the boundary of the tail.

It is important to put the numerous tail-related observations into perspective with other, similar observations. Table 1 is, in fact, a continuation of the table given by *Kurth et al.* [1981], with the major differences being the identification of 'core' regions in the present list versus the identification of events in the solar wind or magnetosphere in the list given by *Kurth et al.* [1981]. We believe that the core events listed in Tables 1 and 2 are, indeed, traversals or entries into the Jovian magnetotail and, hence, may be classed with those identified as magnetosphere events in the earlier paper. The events with no core are, presumably, more appropriately 'solar wind' events in the terminology of the first paper, although this is not as clear as will be discussed below. By drawing these analogies, however, and looking at the complete data set comprising both lists (plus the additional Voyager 1 event described above), we can gain a better picture of the occurrence of the two basic types of events as a function of position with respect to the nominal aberrated tail position.

Figure 5 displays the combined observations of continuum radiation in this paper and those of *Kurth et al.* [1981] and distinguishes between 'core' or 'magnetosphere' events (filled circles) and 'solar wind' events (open circles). The events are located on a coordinate system that is centered on Jupiter and whose principal plane is parallel to the ecliptic. The $\hat{X}$ direction is in the direction of the sun. As in Figure 3, a model tail is overlayed on the plot for comparison. It is clear that the events thought to be direct passages into the magnetotail lie much closer to the nominal position for the tail than do the remaining events consistent with *Lepping et*

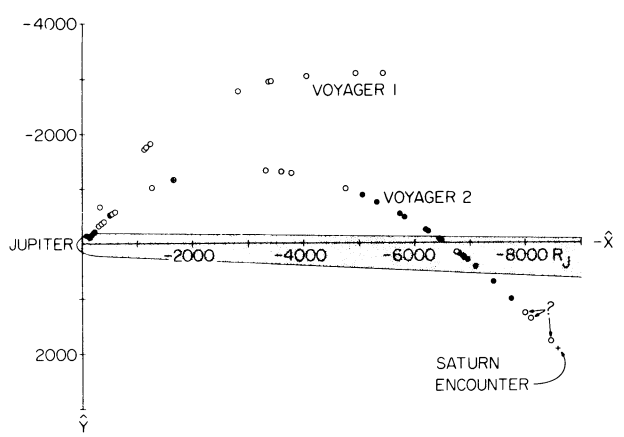

Fig. 5. A summary of the observations of *Kurth et al.* [1981] and those presented herein. The filled circles represent actual detections of the Jovian magnetotail, while the open circles represent observations of continuum radiation that has either escaped into a low-density region of the solar wind or is confined to a wake region near the tail. The + symbols represent detections of the continuum radiation in wideband spectrograms (see text).

al. [1982], who suggest that the actual tail encounters are confined to a 12° (half-angle) cone. It is reasonable to explain the events that are designated with open circles and which are far from the Jupiter-Sun line by using the concept of *Kurth et al.* [1981] of radiation leaking into low-density troughs in the solar wind. Some of the open circles closer to the $-\hat{X}$ axis may be entries into the low-density wake surrounding the tail.

Further evidence that the probability of a tail encounter increases as the nominal tail position is approached is shown in Figure 6. For the analysis illustrated we have attempted to assign a figure of merit to each of the events in Table 2 that takes into consideration both event duration and the depth of the cavity. Hence, in Figure 6 a value proportional to the duration of the event and inversely proportional to the minimum density is plotted on a linear scale versus the angle ϕ. It is clear that the largest values of the contrived figure of merit are centered around 177°, very close to the nominal aberrated position.

The two plus signs in Figure 5 are included as detections of continuum radiation but are distinguished because they are made on the basis of wideband measurements, which are more sensitive than the spectrum analyzer measurements used to compile the data in Table 1 and the table in *Kurth et al.* [1981]. In one case the two types of measurements coincide, and this has aided *Kurth et al.* [1981] in the identification of the continuum radiation. Unfortunately, neither case for which we have wideband coverage corresponds to a low-density core region.

The most distant event designated by a plus symbol in Figure 5 occurred just 2 days before Voyager 2's encounter with Saturn and was just upstream of Saturn's bow shock. Figure 7 is a frequency-time spectrogram showing the evidence for continuum radiation for this event. The diffuse noise with a low-frequency cutoff at 3.5 kHz is characteristic of trapped continuum radiation. The cutoff frequency suggests a local plasma density of 0.15 cm^{-1}. This particular example is very similar to the Voyager 2 event shown in Figure 6 of *Kurth et al.* [1981] at a distance of 2019 R_J. The narrow-band tone at 2.4 kHz and the short burst of noise at 400 Hz plus odd harmonics are spacecraft interference. The tone near 1.75 kHz in Figure 7 is believed to be interference

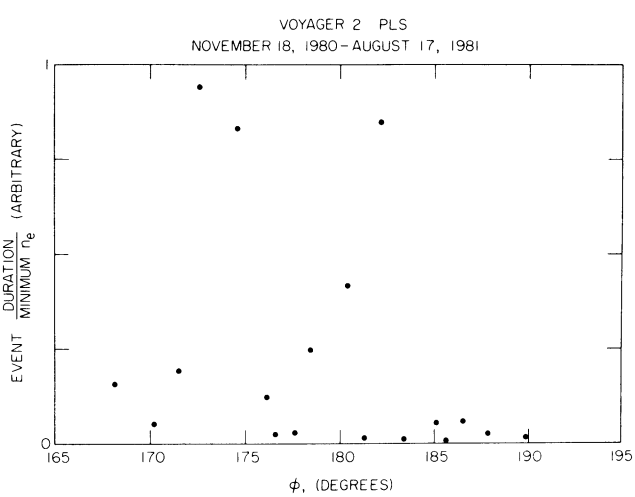

Fig. 6. A plot of a contrived figure of merit (see text) for each of the events listed in Table 2, showing tail encounters with longest durations and lowest minimum densities are clustered near the antisolar direction.

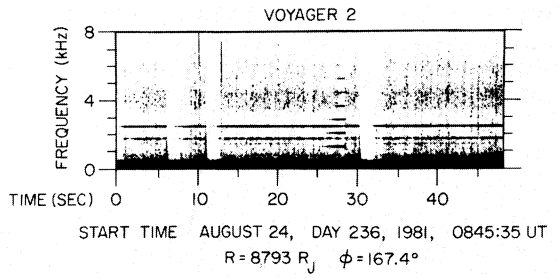

Fig. 7. Continuum radiation detected just upstream from the Saturnian bow shock. Since Saturn does not appear to be the source of diffuse continuum radiation at frequencies above a few kiloHertz, this data implies the Jovian tail was very close to Saturn just prior to the Voyager 2 encounter.

and is thought to be the emission responsible for the three questionable continuum radiation events at the end of Table 1. The source of this interference tone is currently unknown, but we feel certain it enters through the antenna used in common with the planetary radio astronomy instrument. The interference is at a frequency which is probably within the passband of the 1.2-kHz planetary radio astronomy channel used by Lepping et al., and hence we suggest caution be used in the interpretation of their events numbered 7 and 8 as well.

Kurth et al. [1982] have studied in detail the plasma wave data subsequent to those presented in Figure 7, that is, during the Voyager 2 Saturn encounter, and have argued that some of the continuum radiation detected within Saturn's magnetosphere could possibly have originated at Jupiter. While inconclusive, considerable evidence exists that is consistent with the immersion of the Saturnian system in the Jovian tail during the encounter, hence, the most distant '+' symbol in Figure 5 may represent a core event occurring during the Saturn encounter.

Interpretation of the Distant Observations of Jovian Continuum Radiation

In this section we shall attempt to lay out a self-consistent interpretation of the observations of continuum radiation and the simultaneous plasma measurements at large distances downstream from Jupiter. First, we shall look at the new data presented in this paper and suggest a simple explanation of the continuum radiation events taken individually and argue that the 'core' regions are, indeed, passages through at least a portion of the distant Jovian magnetotail. Second, we examine all the observations presented here and in *Kurth et al.* [1981] in order to piece together a gross overview of the possible distant tail structure.

Model for an Individual Tail Encounter

The majority of the events listed in Table 1 are similar to those depicted in Figures 1 and 2 and consist of a broad region of moderately low densities, typically 3×10^{-2} cm^{-3} with one or more 'core' regions of much lower density ($\sim 3 \times 10^{-3}$ cm^{-3}) and with durations of about a day or less. We suggest the most likely interpretation is that the core regions are actual encounters with the distant Jovian magnetotail or part thereof and the surrounding, moderately low density regions are the magnetosheath, or perhaps more appropriately, the wake. We prefer the term wake since one might argue that the magnetosheath extends to the bow shock, which is noticeably absent in these observations and may be

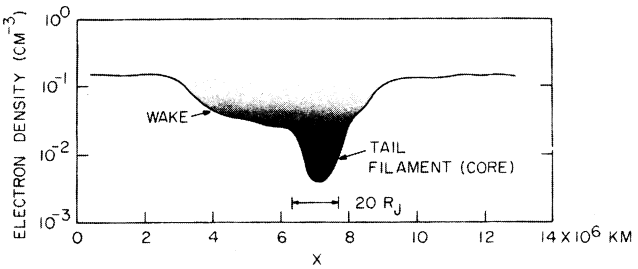

Fig. 8. A schematic representation of a tail encounter. The shading represents continuum radiation trapped in the low-density magnetotail and spilling out into a moderately low density wake region surrounding the tail. While this figure suggests the encounter is actually with just a filament, the data are also consistent with an entry into a well-formed, singular tail (see text).

far removed from the Jupiter-sun line or so weak as to be undetectable.

There are a number of arguments favoring the interpretation of the core events as tail encounters. *Scarf et al.* [1981*b*] argued that the February 1981 event (event 12) was a tail encounter, on the basis of both plasma and plasma wave measurements. We present several more here. The first line of argument is simply one of geometry. Even though all but a very few of the events lie outside of the model tail shown in Figures 3 and 5, the core events in Table 1 all lie reasonably close to the nominal aberrated tail position, and it would not take extraordinary expansions or deflections of the tail to account for most of them. Also, the duration of the core events maximized near $\phi = 180°$. Since Voyager 1 has not detected continuum radiation after the last event plotted in Figure 5, it is apparent that these events are intimately associated with the region downstream from Jupiter and are not characteristic of the solar wind beyond 5 AU in general. Second, there was reasonable expectation that the tail extends ~9000 R_J downstream [*Scarf*, 1979, and references therein], hence the discovery of such an extended tail is not surprising. Third, the analysis of the magnetic fields associated with the core regions show the field to be oriented in the general direction of Jupiter, and a detailed study of the February 1981 event shows a symmetric field signature with a bipolar field in its central region [*Lepping et al.*, 1982]. Lepping et al. conclude that the character of the fields during the events (and, in particular, the February event) are consistent with either a tail or a tail filament interpretation.

The remaining argument favoring the interpretation of the continuum radiation events as tail encounters forms the very basis for this study, which relies almost entirely on the use of the radiation as a tracer for the Jovian magnetosphere. This rationale has been given in detail by *Kurth et al.* [1981], so we shall only briefly review the line of reasoning here. The key lies in the fact that planetary magnetospheres are the only apparent sources of the diffuse nonthermal radiation studied herein. Since the radiation is usually detected at frequencies well below the nominal solar wind plasma frequency, the existence of a low-density path between the planetary source and the spacecraft is implied. At the heliocentric radial distances of Jupiter and Saturn, the Parker spiral direction is approaching 90° with respect to radial, hence most solar wind structures would not be expected to align in the antisolar direction from Jupiter. One might argue that some of the radiation has its source at Saturn, but this still requires a radial structure such as the Jovian tail to provide the low-density path to the spacecraft since Voyager 1 detected no continuum radiation upstream of Saturn at a time when it was not likely for Saturn to be in Jupiter's tail. The presence of 10-hour periodicities in the continuum radiation amplitude noted in some cases also implies a source at Jupiter.

The wake region is an ill-defined region, since there is little to distinguish it from the normal solar wind. Plasma measurements reveal densities, temperatures, and flows that are not unlike low-density regions of the solar wind. For the February 1981 event (event 12), Lepping et al. report southward-draping magnetosheath fields for $\frac{3}{4}$-day intervals before and after the core event; on this basis they suggest that the wake region is very similar to a magnetosheath. We can only speculate that the low densities in the wake regions are due to geometrical shadowing or some other solar wind-tail interaction. We do not feel compelled to characterize the wake regions rigidly until further studies of the plasma and magnetic fields within them are complete.

In Figure 8 we give a stylized sketch of a typical tail interaction region showing both the wake and core areas. The shading represents trapped continuum radiation and is darkest in the core region where the radiation is most intense and extends to the lowest frequencies. In this illustration we have labeled the core region as a tail filament, which we immediately point out is only one possibility. The size scale on the abscissa is based on the assumption that the structure was stationary in the Jupiter-centered system, and the component of the spacecraft velocity perpendicular to the structure (~10 km/s) is the only relevant velocity. Hence, the width of the filament is solely determined by the duration of the core event—in this case about a day. Strictly speaking, this is not a lower limit to the width, since the velocity of the filament could conceivably track the spacecraft. We suggest, however, that this is probably as unlikely as a motionless filament and, therefore, believe filaments on the order of 10 R_J in width are perhaps the smallest structures to be considered. It is more likely that the filament is moving across the spacecraft with a much larger velocity than 10 km/s, since some motion (including expansion) was obviously necessary to put the tail or filament in a position to be observed, and hence it could be much larger than 10 R_J. A schematic of the geometry of this type of tail encounter is given by Lepping et al. in the lower panel of their Figure 4.

An alternate possibility is that the distant tail is well formed and singular, that is, not filamented. In this case the tail would have to expand to envelop the spacecraft and then contract to its nominal size, or, move from its nominal position to one which is in the direction of Voyager. Obviously, there are an infinite number of combinations of these two explanations that are consistent with the observations. This interpretation is similar to the geometry suggested by the construction in the upper panel of Figure 4 of Lepping et al. *Kurth et al.* [1981] discuss several mechanisms for moving the tail from its nominal position, including nonradial solar wind flows and azimuthal pressure gradients. An additional mechanism is suggested by the general geometry of the tail, where the external field is essentially solenoidal and surrounds a longitudinal field imbedded in a plasma column. This is reminiscent of the geometry for the kink instability. The wavelength of the instability would be $\gtrsim 14$ times the radius of the plasma column [*Jackson*, 1962] or about 2700 R_J, which is consistent with the size-scale of the deflections observed.

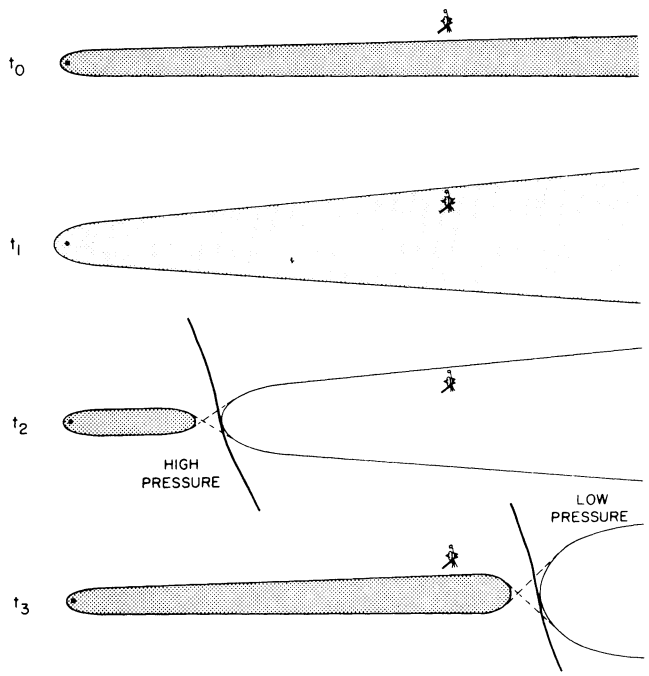

Fig. 9. A series of sketches offering a possible interpretation of event 14 (see Figure 4) in which the continuum radiation disappears long before the spacecraft leaves the region of the low-density tail. The shading represents the presence of continuum radiation and is noticeably absent in the disconnected tail because the low-density path or waveguide has been interrupted at the pinch-off by high densities.

Preliminary analyses of the plasma observations favor the expanding tail mechanism. There is considerable evidence of a correlation between solar wind conditions and the occurrence of tail encounters. A brief glance at Tables 1 and 2 reveals a tendency for events to occur roughly a month apart and, Lepping et al. report a periodicity of 26.5 days between events. This is so close to the solar rotation period that further formal analysis will almost certainly show a real relationship. In fact, it would be reasonable to expect a direct solar wind influence on such a large, tenuous structure so distant from its source. Analysis of the plasma data indicates events are often observed at the trailing edges of solar wind streams where the ram pressure minimizes. Hence, it is clear that the tail sightings could very easily be associated with an expanded tail in response to a decrease in the external pressure. Further analysis of the plasma data leading to a better understanding of the solar wind's control of the tail is the subject of a forthcoming paper.

One theoretical question that will have to be examined before a good understanding of extended tail dynamics is in hand will be the stability of such a structure. Clearly, if tail expansion is accompanied by decreasing magnetic field strength, as appears to be the case for most of the events (R. P. Lepping, private communication, 1982), then one would expect to see an increase in the internal plasma pressure to maintain overall pressure balance. Such pressure increases are not observed, although sufficient numbers of >6-keV ions and electrons could be present to provide the balance and yet not be detected by the PLS instrument. For example, a component with a density of $\sim 10^{-3}$ cm^{-3} and a temperature of ~10 keV would be sufficient to provide pressure balance; this component, if present, could be the remnant of the magnetospheric wind from Jupiter [*Krimigis et al.*, 1981]. It is also possible that there is sufficient tension in the magnetic field to balance the lateral forces. That is, the magnetic field configuration at the tail boundary with a 90° rotation in the typical orientation may provide a further stabilizing influence on the tail.

The event shown in Figure 4 (event 14 in Tables 1 and 2) is typical of many of the events listed, in that it showed a great disparity in the duration of the continuum radiation event versus that of the density depression obtained by PLS. The reconciliation of these two observations seemed to require a mechanism to 'turn off' the radiation, presumably by imposing a high-density barrier between the source of the radiation and the spacecraft. Figure 9 is a schematic illustration of a process that could explain the observations in Figure 4. At time t_0 the spacecraft is well outside the normal tail and monitors the usual solar wind conditions. At time t_1 the solar wind ram pressure has decreased near the trailing edge of a solar wind stream, the tail has expanded, enveloping the spacecraft, and continuum radiation can be detected. At time t_2 a high-pressure region in the solar wind has pinched off the tail at some distance downstream from Jupiter, yet still upstream from the spacecraft. The pinch-off is characterized by higher densities, and the continuum radiation that propagates down the tail at the speed of light turns off almost instantaneously. Meanwhile, the spacecraft is still in the low-density region of the now-detached tail; hence, the PLS and magnetometer measurements continue to show low densities and taillike field configurations. Finally, at t_3 the high-pressure region has passed the spacecraft and it is again outside the tail monitoring nominal solar wind conditions.

For the example in Figure 4, t_2 occurs near the beginning of day 73 when the continuum radiation disappears. Perhaps the earliest time for the passage of the high-pressure region t_3 is day 79, although the density and field strength continue to increase until about day 83. Assuming, however, that $t_3 - t_2 \approx 6$ days, and also assuming a propagation speed of about 400 km/s for the solar wind, the pinch-off had to have occurred ~3000 R_J upstream from the spacecraft or about 3500 R_J downstream from Jupiter. There is no way to check the validity of this proposed sequence of events, however, it is comforting that the proposed pinch-off occurred at a realistic position, i.e., between Jupiter and the spacecraft.

The preceding scenario is inspired in large part from plasma tail disconnection events in comets [*Niedner et al.*, 1978; *Niedner and Brandt*, 1978; *Ip and Mendis*, 1978]. Quite simply, it is thought that the passage of an interplanetary sector boundary over a comet results in magnetic field line reconnection. Photographs of comets have often shown evidence for the total disconnection of the plasma tail and subsequent growth of a new one. *Niedner and Brandt* [1978] apply this theory to a tail disconnection event of comet Kohoutek 1973f and demonstrate a good temporal correlation with the passage of the magnetic field sector boundary. Similar, although not necessarily identical, processes should be considered for extended planetary magnetotails. Variations of the tail disconnection events in comets can be generated which can explain observations of the low-density magnetotail with the complete absence of continuum radiation simply by decreasing the time between the tail expansion and pinch-off so that the disconnection has occurred before the distant tail has expanded. It is interesting that Lepping et al. indicated that there was evidence for the passage of a sector boundary during event 12, which also

exhibited a long delay between the disappearance of continuum radiation and a return to higher solar wind densities.

Admittedly, the explanation of event 14 by a complete tail disconnection is highly speculative, but similar dynamics have been suggested for the terrestrial magnetotail (see, for example, *Birn and Hones* [1981], where computer modeling of dynamic reconnection in the earth's tail predicts the formation of a 'magnetic bubble' or 'plasmoid' that moves tailward from the X line). The formation of 'magnetic bubbles' implies density variations along the tail, which might provide a high-density barrier to electromagnetic waves without requiring a complete disconnection of the tail.

Implications for the Gross Structure of the Jovian Tail

Figure 5 presents a rather large set of observations bearing on the gross structure of the Jovian magnetotail. If we assume the filled circles in the figure represent actual entries into the magnetotail and the open circles some less-direct detection, we can first confirm what most would have been willing to assume a priori—that the tail extends a large distance (>9000 R_J) in the general downstream direction. As first noted by *Kurth et al.* [1981] and confirmed here, the encounters may occur far from the expected position of the tail, given a purely radial solar wind without azimuthal pressure gradients.

Between the final magnetosphere encounter reported by *Kurth et al.* [1981] at 706 R_J and the first core event reported herein at 5108 R_J there are a large number of continuum radiation events (denoted by open circles in Figure 5) that are evidently not direct observations of the Jovian magnetotail. *Kurth et al.* [1981] explained these as being continuum radiation generated within the Jovian magnetosphere and as having escaped the magnetospheric cavity via a low-density solar wind trough acting as a waveguide or light pipe. We believe this to be a valid explanation, particularly for those events well off the Jupiter-sun line. As the trajectory of Voyager 2 swings back into the downstream direction, though, we suggest that the noncore events may also be interpreted as close brushes with the tail but without actual penetration. The low-density regions defined by these events, then, are not just low-density structures in the solar wind but actual wake regions associated with the solar wind-tail interaction.

It is difficult to determine an upper limit to the nominal width of the tail on the basis of the data presented herein, although from Figures 3 and 5 it is apparent that a tail normally >1000 R_J wide is much too large, since Voyager 2 would have been in the tail for a much longer, more continuous interval. We suspect, then, a tail width of several hundred Jupiter radii would be more reasonable. It is possible, though, that temporary expansions of the tail might explain some of the sightings. It is also difficult to rule out a filamented tail; however, the individual filaments would have to be on the order of 10 R_J, or larger, in width. If the tail were highly filamented with many smaller structures, several very brief (a few minutes) encounters would have been observed, and there is no evidence for these. *Kurth et al.* [1981] have suggested the Jovian magnetotail may have a structure similar to the plasma tails of comets, and in fact, photographs of the plasma tails of many comets often show a few (less than 10) distinct tail filaments, cf., *Brandt and Mendis* [1979].

The plasma wave data offer one possible method of determining an upper bound to the cross-sectional area of the tail. If one assumes (1) that the source of continuum radiation is near Jupiter, (2) that the tail is lossless for electromagnetic waves within the tail at frequencies below the solar wind plasma frequency, and (3) that eventually the tail extends to a downstream position where the wave frequency is greater than the solar wind plasma frequency so that waves escape into free space, then the Poynting flux will vary inversely with the cross-sectional area of the tail (whether it is singular or filamented). For example, if one assumes the model tail shown in Figure 5 in which the width is proportional to the heliocentric radial distance, then one would expect the Poynting flux to be smaller by a factor of $(8.5\text{AU}/5.2\text{AU})^2$ or 2.67 for a flux measurement 7000 R_J downstream versus one very near Jupiter (~100 R_J). The voltage spectral density at 562 Hz was measured for the core event on day 108 of 1981 (at 6950 R_J) and found to be $\sim 2 \times 10^{-12}$ $V^2m^{-2}Hz^{-1}$. Typical values at the same frequency in the near-Jupiter tail are ~100 times larger, near 2×10^{-10} $V^2m^{-2}Hz^{-1}$. If the assumptions are correct, this would imply that the width of the tail at 7000 R_J is 10 times that near Jupiter, or in the range of ~2000–4000 R_J. Clearly, if the tail were this large, Voyager would have been in the tail continuously over the time period represented in Figure 3. Therefore, one or more of the assumptions used in this estimate is false. *Kurth et al.* [1981] have shown that there are radiation leaks into low-density solar wind troughs, hence, it is unreasonable to expect the tail to be lossless. The disparity between a decrease in flux of 10^2 versus 2.67 is probably a combination of a (temporarily) larger-than-expected tail cross section and various factors such as leaks, which make the tail a lossy radiation cavity. Note, however, that the reduction in flux assuming R^{-2} free-space propagation (corresponding to a perfectly lossy cavity) would be on the order of 5×10^{-3} at a distance of ~7000 R_J; hence, the tail partially confines the radiation. That is, even though the tail is a lossy cavity, it is not totally so.

CONCLUSIONS

Voyager 2 plasma wave and plasma observations have provided evidence for an extended Jovian magnetotail of at least 8800 R_J in length. Tail-related phenomena, particularly nonthermal continuum radiation, are observable over vast regions of interplanetary space beyond the orbit of Jupiter and are not narrowly confined to the antisolar direction. We briefly summarize our conclusions about the distant Jovian magnetotail, as follows:

1. The tail was encountered on numerous occasions over the span of several months, and in a wide range of locations, implying a highly dynamic structure and/or a tail with several filaments.

2. Tail encounters occurred quasi-periodically, approximately once per month, implying direct solar wind control.

3. Several entries into the tail occurred at the trailing edge of solar wind streams when the ram pressure was a minimum, suggesting simple tail expansion could explain the sightings, although deflection of the tail is also consistent with the observations. (We note, however, that current evidence from the plasma and magnetometer investigations for the pressure balance required for an expanding tail does not exist unless there is a hotter plasma present that would not be observable by the plasma instrument.)

4. Encounters with the Jovian tail showed the deepest

density minima, longest durations, and highest occurrence probability near the nominal aberrated tail position.

5. Some evidence for large-scale waves in the tail or on the tail boundary was found. A typical period for these waves was 2–2 $\frac{1}{2}$ days.

6. The existence of tail structures without the presence of continuum radiation may be explained by the existence of a high-density barrier to electromagnetic radiation between Jupiter and the spacecraft and may be evidence of reconnection in the tail or a detached tail similar to tail disconnection events in comets.

7. Some observations of continuum radiation well off the Jupiter-sun line can be explained by leakage into low-density solar wind troughs acting as waveguides.

8. The Jovian tail or tail filament appears to have a fairly well-defined structure. The core or actual tail is characterized by low densities ($n_e < 10^{-2}$ cm^{-3}) and radially aligned (toward or away from Jupiter) bipolar fields [*Lepping et al.*, 1982]. The surrounding wake is composed of solar windlike plasma with $n_e \sim 3 \times 10^{-2}$ cm^{-3} and has a sheathlike field configuration [*Lepping et al.*, 1982].

Acknowledgments. The authors would like to express their gratitude to R. P. Lepping for a number of useful discussions and comments, to the Voyager magnetometer team at Goddard Space Flight Center for the use of magnetic field data prior to publication, and to M. D. Desch for his help in the preparation of Figure 4. The research at the University of Iowa was supported by NASA through contract 954013 with the Jet Propulsion Laboratory, by TRW subcontract M16607DB1S, by grants NAGW-337 and NGL-16-001-043 with NASA Headquarters, and by the Office of Naval Research. The research at TRW was supported by NASA through contract 954012 with JPL and grant NASW-3504 from NASA Headquarters. Research at MIT was supported by NASA through contract 953733 with JPL.

The Editor thanks M. D. Desch and R. P. Lepping for their assistance in evaluating this paper.

REFERENCES

Birn, J., and E. W. Hones, Jr., Three-dimensional computer modeling of dynamic reconnection in the geomagnetic tail, *J. Geophys. Res.*, *86*, 6802, 1981.

Brandt, J. C., and D. A. Mendis, The interaction of the solar wind with comets, in *Solar System Plasma Physics*, vol. 2, edited by C. F. Kennel, L. J. Lanzerotti, and J. N. Parker, pp. 253–292, North-Holland, Amsterdam, 1979.

Bridge, H. S., J. W. Belcher, R. J. Butler, A. J. Lazarus, A. M. Mavretic, J. D. Sullivan, G. L. Siscoe, and V. M. Vasyliunas, The plasma experiment on the 1977 Voyager mission, *Space Sci. Rev.*, *21*, 259, 1977.

Grzedzielski, S., W. Macek, and P. Oberc, Expected immersion of Saturn's magnetosphere in the Jovian magnetic tail, *Nature*, *292*, 615, 1980.

Gurnett, D. A., W. S. Kurth, and F. L. Scarf, Plasma wave observations near Jupiter: Initial results from Voyager 2, *Science*, *206*, 987, 1979.

Gurnett, D. A., W. S. Kurth, and F. L. Scarf, The structure of the Jovian magnetotail from plasma wave observations, *Geophys. Res. Lett.*, *7*, 53, 1980.

Ip, W.-H., and D. A. Mendis, The flute instability as the trigger mechanism for disruption of cometary plasma tails, *Astrophys. J.*, *223*, 671, 1978.

Jackson, J. D., *Classical Electrodynamics*, John Wiley, New York, 1962.

Krimigis, S. M., J. F. Carbary, E. P. Keath, C. O. Bostrom, W. I. Axford, G. Gloeckler, L. J. Lanzerotti, and T. P. Armstrong, Characteristics of hot plasma in the Jovian magnetosphere: Results from the Voyager spacecraft, *J. Geophys. Res.*, *86*, 8227, 1981.

Kurth, W. S., D. A. Gurnett, F. L. Scarf, R. L. Poynter, and J. D. Sullivan, Voyager observations of Jupiter's distant magnetotail, *J. Geophys. Res.*, *86*, 8402, 1981.

Kurth, W. S., F. L. Scarf, J. D. Sullivan, and D. A. Gurnett, Detection of nonthermal continuum radiation in Saturn's magnetosphere, *Geophys. Res. Lett.*, *9*, 889, 1982.

Lepping, R. P., L. F. Burlaga, M. D. Desch, and L. W. Klein, Evidence for a distant (>8700 R_J) Jovian magnetotail: Voyager 2 observations, *Geophys. Res. Lett.*, *9*, 885, 1982.

Niedner, M. B., and J. C. Brandt, Interplanetary gas, 23, Plasma tail disconnection events in comets: Evidence for magnetic field line reconnection at interplanetary sector boundaries?, *Astrophys. J.*, *223*, 655, 1978.

Niedner, M. B., E. D. Rothe, and J. C. Brandt, Interplanetary gas, 22, Interaction of comet Kohoutek's ion tail with the compression region of a solar-wind corotating stream, *Astrophys. J.*, *221*, 1014, 1978.

Scarf, F. L., Possible traversals of Jupiter's distant magnetic tail by Voyager and Saturn, *J. Geophys. Res.*, *84*, 4422, 1979.

Scarf, F. L., and D. A. Gurnett, A plasma wave investigation for the Voyager mission, *Space Sci. Rev.*, *21*, 289, 1977.

Scarf, F. L., D. A. Gurnett, and W. S. Kurth, Jupiter plasma wave observations: An initial Voyager 1 overview, *Science*, *204*, 991, 1979.

Scarf, F. L., D. A. Gurnett, and W. S. Kurth, Measurements of plasma wave spectra in Jupiter's magnetosphere, *J. Geophys. Res.*, *86*, 8181, 1981*a*.

Scarf, F. L., W. S. Kurth, D. A. Gurnett, H. S. Bridge, and J. D. Sullivan, Jupiter tail phenomena upstream from Saturn, *Nature*, *292*, 585, 1981*b*.

Scarf, F. L., D. A. Gurnett, W. S. Kurth, and R. L. Poynter, Voyager 2 plasma wave observations at Saturn, *Science*, *215*, 587, 1982.

(Received June 30, 1982;
revised September 8, 1982;
accepted September 9, 1982.)